

DNA methylation and survival differences associated with the type of IDH mutation in 1p/19q non-codeleted astrocytomas

Survival associated with IDH mutation-type

C Mircea S Tesileanu¹, Wies R Vallentgoed¹, Marc Sanson², Walter Taal¹, Paul M Clement³, Wolfgang Wick⁴, Alba Ariela Brandes⁵, Jean Francois Baurain⁶, Olivier L Chinot⁷, Helen Wheeler⁸, Sanjeev Gill⁹, Matthew Griffin¹⁰, Leland Rogers¹¹, Roberta Rudà¹², Michael Weller¹³, Catherine McBain¹⁴, Jaap Reijneveld¹⁵, Roelien H Enting¹⁶, Francesca Caparrotti¹⁷, Thierry Lesimple¹⁸, Susan Clenton¹⁹, Anja Gijtenbeek²⁰, Elisabeth Lim²¹, Filip de Vos²², Paul J Mulholland²³, Martin J B Taphoorn²⁴, Iris de Heer¹, Youri Hoogstrate¹, Maurice de Wit¹, Lorenzo Boggiani¹, Sanne Venneker²⁵, Jan Oosting²⁵, Judith VMG Bovée²⁵, Sara Erridge²⁶, Michael A Vogelbaum²⁷, Anna K Nowak^{28,29,30}, Warren P Mason³¹, Johan M Kros³², Pieter Wesseling³³, Ken Aldape³⁴, Robert B Jenkins³⁵, Hendrikus J Dubbink³², Brigitta Baumert^{36,37}, Vassilis Golfinopoulos³⁸, Thierry Gorlia³⁸, Martin van den Bent¹ and Pim J French¹

¹Dept Neurology, Brain Tumor Center at Erasmus MC Cancer Institute Rotterdam, the Netherlands

²Sorbonne Universités UPMC Univ Paris 06, Inserm, CNRS, AHP, Institut du cerveau et de la moelle (ICM)- Hôpital Pitié-salpêtrière, Boulevard de l'hôpital, F-75013, Paris, France

³Department of Oncology, KU Leuven and Department of General Medical Oncology, UZ Leuven, Belgium

⁴Neurologische Klinik und Nationales Zentrum für Tumorerkrankungen Universitätsklinik, Heidelberg, Germany

⁵Medical Oncology Department, AUSL-IRCCS Scienze Neurologiche, Bologna Italy

⁶Medical Oncology Department, King Albert II Cancer Institute, Cliniques universitaires Saint-Luc, Université Catholique de Louvain, Bruxelles, Belgium

⁷Aix-Marseille University, AP-HM, Neuro-Oncology division, Marseille, France

⁸Northern Sydney Cancer Centre, St Leonards, NSW 2065 Australia: University of Sydney

⁹Dept Medical Oncology, Alfred Hospital, Melbourne, Australia

¹⁰Department of Clinical Oncology, Nottingham University Hospitals NHS Trust, Nottingham, UK

¹¹Department of Radiation Oncology, Barrow Neurological Institute, Phoenix AZ USA

¹²Department of Neuro-Oncology, City of Health and Science Hospital and University of Turin, Italy

¹³Department of Neurology and Brain Tumor Center, University Hospital and University of Zurich, Zurich, Switzerland

¹⁴Department of Clinical Oncology, The Christie NHS FT, Manchester, UK

¹⁵Brain Tumor Center Amsterdam & Department of Neurology, Amsterdam University Medical Center

¹⁶Department of Neurology, UMCG, University of Groningen, Groningen, the Netherlands

¹⁷Department of Radiation Oncology, University Hospital of Geneva, Geneva, Switzerland

¹⁸Department of Clinical Oncology, Comprehensive Cancer Center Eugène Marquis, Rennes, France

¹⁹Weston Park Hospital, Sheffield, UK

²⁰Department of Neurology, Radboud University Medical Centre, Nijmegen, The Netherlands

²¹Department of Clinical Oncology, PLYMOUTH HOSPITALS NHS TRUST

²²Department of Medical Oncology, UMC Utrecht Cancer Center, Utrecht, the Netherlands

²³University College Hospital, London, UK

²⁴MC Haaglanden, Den Haag, Netherlands

²⁵Department of Pathology, Leiden University Medical Center, Leiden, The Netherlands

²⁶Edinburgh Centre for Neuro-Oncology, Western General Hospital, University of Edinburgh, Edinburgh, UK

²⁷Department of NeuroOncology, Moffitt Cancer Center, Tampa, Florida, USA

²⁸School of Medicine and Pharmacology, University of Western Australia, 35 Stirling, Highway Crawley WA 6009 Australia

²⁹CoOperative Group for NeuroOncology, University of Sydney, Camperdown NSW, Australia

³⁰Department of Medical Oncology, Sir Charles Gairdner Hospital, Hospital Avenue, Nedlands WA 6009 Australia

³¹Princess Margaret Cancer Centre, University of Toronto, Toronto, Canada

³²Department of Pathology, Erasmus University Medical Center, Rotterdam, the Netherlands

³³Department of Pathology, VU University Medical Center, Amsterdam, The Netherlands

³⁴Princess Margaret Cancer Centre, University of Toronto

³⁵Department of Laboratory Medicine and Pathology, Mayo Clinic, Rochester MN, USA

³⁶Dept. Radiation-Oncology (MAASTRO), Maastricht University Medical Center (MUMC) and GROW (School for Oncology), Maastricht, Netherlands;

³⁷Institute of Radiation-Onology, Chur, Switzerland

³⁸EORCT HQ, Brussels, Belgium

Single sentence summary: Astrocytoma patients with tumours harbouring IDH mutations other than p.R132H have increased DNA methylation levels and longer survival

Abstract

Somatic mutations in the isocitrate dehydrogenase genes *IDH1* and *IDH2* occur at high frequency in several tumour types. Even though these mutations are confined to distinct hotspots, we show that gliomas are the only tumour type with an exceptionally high percentage of IDH1^{R132H} mutations. This high prevalence is important as IDH1^{R132H} is presumed to be relatively poor at producing D-2-hydroxyglutarate (D-2HG) whereas high concentrations of this oncometabolite are required to inhibit TET2 DNA demethylating enzymes. Indeed, patients harbouring IDH1^{R132H} mutated tumours have lower levels of genome-wide DNA-methylation, and an associated increased gene expression, compared to tumours with other IDH1/2 mutations (“non-R132H mutations”). This reduced methylation is seen in multiple tumour types and thus appears independent of site of origin. For 1p/19q non-codeleted glioma patients, we show that this difference is clinically relevant: in samples of the randomised phase III CATNON trial, patients harbouring non-R132H mutated tumours have better outcome (HR 0.41, 95% CI [0.24, 0.71], p=0.0013). Non-R132H mutated tumours also had a significantly lower proportion of tumours assigned to prognostically poor DNA-methylation classes (p<0.001). IDH mutation-type was independent in a multivariable model containing known clinical and molecular prognostic factors. To confirm these observations, we validated the prognostic effect of IDH mutation type on a large independent dataset. The observation that non-R132H mutated 1p/19q non-codeleted gliomas have a more favourable prognosis than their IDH1^{R132H} mutated counterpart is clinically relevant and should be taken into account for patient prognostication.

Keywords

Astrocytoma; D-2-hydroxyglutarate; oligodendroglioma; acute myeloid leukemia; chondrosarcoma; genome wide DNA methylation; gene expression; survival; IDH1; IDH2; p.R132H

Introduction

Somatic mutations in the isocitrate dehydrogenase genes *IDH1* and *IDH2* occur at high frequency in various tumour types including gliomas (primary malignant central nervous system tumours), intrahepatic cholangiocarcinomas (bile duct tumours), enchondromas and chondrosarcomas (bone tumours), sinonasal undifferentiated carcinomas and leukemias^{1,2}. More sporadic but similar mutations have been found in a wide variety of other tumour types including melanoma, prostate and pancreatic cancer³. *IDH1/2* mutations are causal for the disease and tumours often remain dependent on the mutation for growth^{4,5}. The importance of the mutation is confirmed by the activity of IDH-inhibitors: inhibiting the mutant activity of either *IDH1* or *IDH2* shows anti-tumour activity in relapsed/refractory *IDH1/2* mutated acute myeloid leukemia^{6,7} and cholangiocarcinoma patients⁸. The objective response rates in these trials are in the order of 40%, though patients eventually relapse. In gliomas however, mutant *IDH1/2* inhibitors have thus far not shown a survival benefit, but further studies on early-stage tumours are ongoing⁹.

The *IDH1/2* mutations are confined to defined hotspots within the genes that affect either arginine 132 (R132) in *IDH1* or the arginines R172 or R140 in *IDH2*. These mutations change the activity of the wild-type (wt) protein from an enzyme that produces alpha-ketoglutarate (aKG) to an enzyme that produces D-2 hydroxyglutarate (D-2HG)^{1,10}. D-2HG in its turn is a main effector in oncogenesis e.g. by inhibiting aKG-dependent dioxygenases, which keeps cells in an undifferentiated state^{11,12}. Although *IDH1/2* mutations are confined to these three hotspots, several reports have shown that the IDH-mutation spectrum differs per tumour type^{1,13-15}. This difference is interesting as other groups have shown that mutations differ in their ability to produce D-2HG^{16,17}. *IDH1*^{R132H}, the *IDH1/2* mutation with relatively low D-2HG production capacity, is the most common mutation in gliomas; other mutations such as *IDH1*^{R132C} have 10-fold lower K_M and have higher enzymatic efficiency^{16,17}. The differential D-2HG production capacity is supported by observations from cell lines and clinical samples where tumours harbouring the *IDH1*^{R132H} mutation have lower D-2HG levels compared to those with other IDH mutations^{16,18,19}. This difference may have biological implications as not all aKG-dependent enzymes are equally well inhibited by D-2HG^{20,21}.

Here, we have used data from six large and independent DNA methylation datasets (the randomised phase III CATNON clinical trial on anaplastic 1p/19q non-codeleted gliomas²², the TCGA-LGG cohort²³, samples included in the TAVAREC randomised phase 2 clinical trial on 1p/19q non-codeleted gliomas²⁴, a large cohort of acute myeloid leukemias (AML)²⁵ and a cohort of chondrosarcomas (Venneker et al, accepted for publication)) derived from four different tumour types, to examine the molecular effects of different types of *IDH1/2* mutations. We report that tumours harbouring *IDH1*^{R132H} mutations, regardless of tumour type, have lower genome-wide DNA methylation levels compared to those harbouring other ('non-R132H') *IDH1/2* hotspot mutations. For 1p/19q non-codeleted glioma patients, we show this difference has clinical relevance as patients harbouring such non-R132H mutated tumours have improved survival. Our data support the notion that increased genome-wide DNA methylation levels are associated with improved outcome in this tumour type and indicate that the type of *IDH1/2* mutation should be taken into account for prognostication of 1p/19q non-codeleted glioma patients.

Methods

Datasets: The COSMIC database (assessed 27 December 2019) was screened for hotspot *IDH1* (R132) and *IDH2* (R172 and R140) mutations. Mutations were stratified by tumour type; tumours with low prevalence of mutations were concatenated ('other tumours': prostate n=11, pancreas n=6, skin n=32, large intestine n=1, soft tissue n=22, endometrium n=1, breast n=9, urinary tract n=2, liver n=7, stomach n=1, upper aerodigestive tract n=35, salivary gland n=1, thyroid n=1). CATNON clinical data²² and *IDH1/2* mutation and DNA methylation data (Tesileanu, submitted) were reported previously. TCGA glioma data (DNA methylation and RNA-seq)²³, MSK-IMPACT data²⁶ and AML data²⁵ were downloaded from the TCGA data portal. Clinical data and mutation status for the chondrosarcoma data were reported previously (Venneker et al, accepted for publication). Clinical data from the TAVAREC trial were derived from ref²⁴, and supplemented with DNA methylation data of 89 tumours. Most (80%) TAVAREC samples were derived from the initial tumour. Processing of CATNON and TAVAREC DNA methylation data was performed as described (Tesileanu, submitted). For the CATNON, TCGA-astrocytoma and TAVAREC datasets, we included only *IDH1/2* mutated samples from non 1p/19q-codeleted tumours. For *IDH1/2* mutated MSK-IMPACT samples, the distinction between astrocytic and oligodendrocytic tumours was made by absence or presence of telomerase reverse transcriptase (TERT) promoter mutations^{27,28}. In the Chinese Glioma Genome Atlas [CGGA]²⁹, the exact IDH-mutation was not noted and therefore limited for the scope of this analysis. We used only the 1p/19q codeleted tumours in this dataset with *IDH2* mutations being designated as "non-R132H" mutations and all *IDH1* mutations as "R132H". In oligodendrogliomas, IDH1 mutations virtually always result in R132H¹⁴. RNA-seq data (raw read counts) were normalized and processed using DEseq2.

Statistical analysis: Survival curves were created using the Kaplan-Meier method. The log-rank test was used to determine survival differences. A Wilcoxon rank test on beta values (i.e. the intensity of the methylated probe/sum of methylated and unmethylated probe intensity) was used to identify differentially methylated probes in CATNON and TCGA-astrocytoma datasets. To increase power in the smaller sized datasets, we performed an *F*-test on M-values (i.e. the log₂ ratio of the methylated/unmethylated probe intensities) to identify differentially methylated CpGs using the dmpFinder function in the Minfi Bioconductor package³⁰. To further increase statistical power in the chondrosarcoma dataset (required as this dataset had few samples), we first made a selection of the most variable probes (i.e. those with a standard deviation >2; ~5% of the total number of probes) followed by an *F*-test on the M-values. In all differential methylation analysis, p-values were corrected for false discovery rate (adjusted P-value).

Differences in mutation frequencies were determined using a chi squared test. Pathway analysis was performed using Ingenuity pathway analysis (Qiagen, Venlo, the Netherlands). An association model was made with the Cox proportional hazards method and included, next to *IDH1/2* mutation type, factors that are known to be related to outcome from literature such as sex, treatment with temozolomide, age at randomization, WHO performance score, *MGMT* promoter methylation status, use of corticosteroids at randomization, and DNA methylation profiling. All p values below 0.05 were considered significant. Statistical analysis was performed using R version 3.6.3 and packages minfi, stats, rms, survival.

Results

The IDH1^{R132H} mutation predominates in gliomas

We screened the catalogue of somatic mutations in cancer (COSMIC) database³¹, extracted *IDH1/2* hotspot mutation data (*IDH1*^{R132}, *IDH2*^{R172} and *IDH2*^{R140}) and stratified them by tumour organ site. As expected, tumours with a high frequency of *IDH1/2* mutations include central nervous system (CNS), biliary tract, bone, haematopoietic and lymphoid tumours (leukemias). Interestingly, even if there are only three mutational hotspots, there are marked differences in the distribution of mutations between tumour sites (figure 1). For example, the *IDH1*^{R132H} mutation is by far the most predominant *IDH* mutation in CNS tumours (n=7265/8026, 90.5%) whereas this mutation is present at much lower frequencies in bone (n=49/361, 13.6%), leukemic (n=519/2995, 17.3%) and other tumours (n=14/129, 10.9%), and thus far has never been identified in biliary tract tumours (n=212) (p<0.001, chi square test). In contrast, the mutation that results in *IDH1*^{R132C} is quite rare in gliomas (223/8026, 2.8%) but much more prevalent in all other tumour types: bone (n=212/361, 67.1%), leukemic (n=493/2995, 16.5%), biliary tract (n=114/212, 53.8%) and other tumours (n=14/129, 10.9%). This difference is despite the fact that the *IDH1*^{R132H} and the *IDH1*^{R132C} are both the result of a transition mutation (G>A and C>T, respectively). In general, transition mutations are much more common than transversion mutations³². There is also a major difference in the distribution of *IDH2* mutations which are very common in haematopoietic and lymphoid tumours but rare in all other tumour types. Mutations of the R140 in *IDH2* are virtually exclusive to haematopoietic and lymphoid tumours.

DNA methylation is lower in IDH1^{R132H} mutant glioma

Previous reports have shown that D-2HG is a weak inhibitor of TET2 enzymes as relatively high levels of D-2HG are required to inhibit the enzyme^{21,33}. We therefore hypothesized that *IDH* mutations that are presumed to be poor in producing D-2HG (i.e. *IDH1*^{R132H}), produce levels of the oncometabolite that are insufficient to completely inhibit the aKG-dependent dioxygenase TET2. If so, based on the molecular function of TET2 enzymes in mediating the first step in DNA demethylation, *IDH1*^{R132H} mutated tumours may have lower levels of DNA methylation than those harbouring other hotspot *IDH* mutations (“non-R132H” mutations).

To test this hypothesis, we used genome-wide DNA methylation data from CATNON trial samples and compared profiles of *IDH1*^{R132H} mutated tumours (n=369, presumed low D-2HG production) to those harbouring other “non-R132H” *IDH1* and *IDH2* hotspot mutations (n=69, presumed high D-2HG production). Our data shows that the overall level of DNA methylation was significantly lower in tumours harbouring *IDH1*^{R132H} mutations compared to tumours harbouring non-R132H mutations. For example, there are 2461 probes showing a reduction in beta values > 0.2 in *IDH1*^{R132H} mutated tumours (at p<0.01) but there are no probes showing an increase > 0.2. This is exemplified in the volcano plot where a strong skew towards increased DNA methylation in non-R132H mutated samples is observed (figure 2A). Probes showing the largest increase in DNA methylation were those that were partially methylated in *IDH1*^{R132H} mutated tumours (i.e. probes with beta values between 0.25 and 0.75); there were few probes that became (partially) methylated from an unmethylated state (figure 2B).

Gliomas with higher levels of genome wide DNA methylation generally are associated with longer survival in adults^{23,34-36}. Since non-R132H mutated gliomas have increased DNA methylation levels, we compared overall survival of patients with different *IDH* mutations. In patients included in the CATNON randomised phase III clinical trial, those harbouring tumours with non-R132H mutations indeed had

longer overall survival compared to patients harbouring IDH1^{R132H} mutated tumours (**figure 2C**). The hazard ratio for non-R132H mutations was 0.41, 95% CI [0.24, 0.71], $p=0.0013$.

DNA methylation profiling can also assign tumours to specific (prognostic) methylation subclasses. In line with the poorer survival, IDH1^{R132H} mutated tumours also had a significantly higher proportion assigned to the prognostically poorer subclass A_IDH_HG (“IDH-mutant, high grade astrocytoma”, $n=100/366$ v. $9/71$, $p=0.036$, chi-squared test) using the subclasses as defined by Capper et al. (“CNS-classifier”)³⁷. They also have a higher proportion of G-CIMP low tumours ($18/369$ v. $0/62$) and G-CIMP-high tumours with risk to progression to G-CIMP low ($111/335$ v. $2/62$) in the classifier as defined by the TCGA and de Souza et al. (“glioma classifier”, $p<0.001$, chi-squared test, **table 1**)^{23,34}.

A heatmap of the most differentially methylated CpGs of CATNON data ($n=677$, selected on a beta value change >0.25 and false discovery corrected p values $<10e-5$) shows a gradient from high to low methylation levels. As expected, the non-R132H mutated tumours cluster together at the high-methylation end of this spectrum. Interestingly, most of the tumours with less favourable molecular subtypes (A_IDH_HG, G-CIMP low, G-CIMP high with risk to progression) clustered together at the other, demethylated end (**figure 2E**). Although the clinical follow-up of CATNON patients is limited, the number of mortality events also tended to cluster at the demethylated end of the heatmap which suggests that there is a strong correlation between the level of methylation of these 677 probes and survival.

To determine whether the type of mutation is a prognostic factor independent of the DNA methylation subtypes, we stratified these subtypes by *IDH1/2* mutation (IDH1^{R132H} v. non-R132H). Our data show that, even within the prognostic DNA methylation subtypes, patients harbouring non-R132H mutated tumours had a significantly longer survival compared to those harbouring IDH1^{R132H}-mutated tumours, regardless of the classifier used (**figure 2D, supplementary figure 1**). The type of *IDH1/2* mutation was also an independent prognostic factor in a multivariable analysis that included all known factors associated with survival in this trial (treatment, age, corticosteroid use and sex, **supplementary table 1**). It remained significant when DNA methylation subclass was included in this analysis (**table 1, supplementary table 2**). These data demonstrate that the type of *IDH1/2* mutation is an independent factor associated with patient survival.

To confirm these observations, we performed a similar analysis on the *IDH1/2* mutated, 1p/19q non-codeleted glioma patients included in the TCGA dataset²³. Similar to observed in the CATNON dataset, a striking increase in DNA methylation levels was seen in non-R132H mutated tumours compared to those harbouring a IDH1^{R132H} mutation (**figure 3AB**). Also similar was the observation that patients harbouring non-R132H mutated tumours survived significantly longer; the HR of patients harbouring non-R132H mutated tumours ($n=37$) versus IDH1^{R132H}-mutated tumours ($n=177$) was 0.20 (95% CI [0.047, 0.837], $p=0.028$ **figure 3C**). Finally, IDH1^{R132H} mutated tumours also had a higher proportion of tumours assigned to the prognostically poorer G-CIMP low DNA methylation class ($4/116$ v. $0/27$) and a higher number at risk of progression to G-CIMP low ($29/111$ v. $0/24$, $p=0.016$).

DNA methylation generally shows a negative correlation with gene expression, especially when the methylated CpGs are located near the transcriptional start site^{38,39}. We therefore examined whether the reduction in DNA methylation in IDH1^{R132H} mutated tumours is associated with an increase in gene expression in the 1p/19q non-codeleted gliomas present in the TCGA dataset. Indeed, of the genes differentially expressed between IDH mutation types (with >2 fold change in expression level at $p<0.01$

significance level) in astrocytomas, most (157/183, 86%) were upregulated in IDH1^{R132H} mutated tumours (figure 3D, supplementary table 3). Pathway analysis using these 183 genes indicates that genes upregulated in IDH1^{R132H} mutated tumours were involved in cellular movement, cell death and survival, cell-to-cell signalling and interaction and carbohydrate metabolism (supplementary figure 2).

We performed a second validation using 1p/19q non-codeleted samples included in the randomised phase II TAVAREC clinical trial. Again, the vast majority of probes had lower DNA methylation levels in IDH1^{R132H} mutated tumours (n=83) compared to non-R132H mutated tumours (n=11, figure 4A) and the most differentially methylated probes were those partially methylated in IDH1^{R132H} mutated tumours (figure 4B). Moreover, there was a large degree of overlap in differential DNA methylation between CATNON and TAVAREC samples (figure 4C). In TAVAREC, there was no significant difference in survival between patients harbouring IDH1^{R132H} and non-R132H mutated tumours (HR 1.21, 95% CI [0.60, 2.45], P=0.60). This however, may be related to the specific inclusion criteria of this trial: patients were included only when the tumour showed signs of malignant progression at the time of progression (i.e. contrast enhancement on the MRI scan). In this respect it is interesting to note that the percentage of non-R132H mutated tumours was almost two-fold lower in TAVAREC trial samples (13%) compared to CATNON (19%) and TCGA (20%). Although this difference in frequency was not significant, these numbers are in line with the notion that non-R132H mutated tumours have lower frequencies of malignant progression. The small number of patients harbouring non-R132H mutated tumours (n=11) may also mask potential survival differences. A heatmap of most differentially methylated probes shows that non-R132H-mutated tumours and tumours assigned to the prognostically poorer subclass A_IDH_HG clustered at opposite ends of this heatmap (figure 4D). A forest plot of the combined CATNON, TCGA and TAVAREC survival data shows a summary estimate HR for non-R132H mutated tumours of 0.56 with 95% CI [0.37, 0.85], association p=0.006 (figure 4E).

To test whether mutation-dependent DNA methylation differences were restricted to 1p/19q non-codeleted gliomas, we analysed the genome-wide methylation profiles of i) IDH1/2 mutated, 1p/19q codeleted gliomas (TCGA) ii) acute myeloid leukemias (TCGA) and iii) chondrosarcomas. Although the sample sizes of these datasets were relatively small in all tumour types (1p/19q codeleted gliomas n=135 v. 14; acute myeloid leukemias n=4 v. n=24; chondrosarcomas n=3 v. n=17 for IDH1^{R132H} and non-R132H mutated tumours respectively), there was less DNA methylation in IDH1^{R132H} v. non-R132H mutation tumours (figure 5A-C). These data demonstrate that the level of DNA methylation is lower in tumours harbouring IDH1/2 mutations with presumed low D-2HG production.

Gene expression analysis of 1p/19q codeleted gliomas present in the TCGA dataset identified 148 differentially expressed genes (expression fold change >1 or <-1 and p< 0.01). Similar to observed in astrocytic tumours, the majority of identified genes (123/148, 83%) were upregulated in IDH1^{R132H} mutated tumours (supplementary table 4). Moreover, there was a relatively large degree of concordance in differential expression between the two analyses (figure 5D) and sixteen genes were identified in both analyses.

The number of samples and events of the various datasets in patients with 1p/19q codeleted gliomas was insufficient to determine mutation type dependent survival differences. For example, there were only 14 non-R132H mutated 1p/19q codeleted tumours in the TCGA dataset, with only 1 event noted (in the IDH1^{R132H} mutated tumours there were 14 events in 135 patients). The HR for TCGA samples

was 0.59 (95% CI [0.077, 4.595], $p=0.62$, figure 5E). Also in the MSK-Impact²⁶ and the Chinese Glioma Genome Atlas (CGGA)²⁹ there were too few samples and events to determine survival benefit in patients harbouring non-R132H-mutated tumours. In these datasets, the events/number in non-R132H v. IDH1^{R132H} mutated samples was 0/6 v. 3/34 and 0/5 v. 3/31 in MSK impact, and CGGA datasets respectively. We were not able to determine survival differences in AML (n=12 with 5 events v. n=89, 54 events, HR 1.49, 95%CI[0.59, 3.75], $p=0.39$, figure 5F).

Discussion

Our data shows that *IDH1/2mt* gliomas are distinct when compared to other *IDH1/2mt* tumours in that they have a disproportionately high percentage of $IDH1^{R132H}$ mutations and raise the attractive clinical association between different rarer (codon 132) mutations and outcome. Patients harbouring $IDH1^{R132H}$ mutated tumours have lower levels of genome-wide DNA methylation, regardless of tumour type (1p/19q non-codeleted gliomas, 1p/19q codeleted gliomas, AML and chondrosarcomas). For 1p/19q non-codeleted *IDH1/2mt* gliomas, this difference is clinically relevant as patients harbouring non-R132H mutated tumours have improved outcome. Since $IDH1^{R132H}$ mutations are presumed to be relatively poor in D-2HG production, our data are in line with the observation that glioma patients with higher D-2HG levels have improved outcome⁴⁰. Our data are also in line with data from a meeting abstract showing similar mutation-specific survival differences⁴¹

The observation that patients harbouring non-R132H mutated gliomas have longer survival is of importance for clinical practice as the specific *IDH1/2* mutation could alter patient prognostication. In this respect diagnostic assays should be able to discriminate between the type of IDH-mutation present; non-R132H mutations comprise of up to 20% of all IDH-mutations in 1p/19q non-codeleted gliomas. Moreover, the efficacy of treatment with alkylating agents, *IDH1/2* inhibitors, or other novel treatments might vary per mutation type, and therefore may be taken into account as stratification factor in future clinical trials.

It has been reported that D-2HG is a relatively weak inhibitor of TET2. In fact, the IC50 value for TET2 inhibition (~5 mM) is in the same range as the intratumoural D-2HG levels^{18,33,42,43}. As TET2 mediates the first step in DNA demethylation, lower D-2HG levels may result in reduced inhibition of DNA-demethylation. Such lower D-2HG levels have been reported for $IDH1^{R132H}$ mutated tumours in some studies^{18,43,44} (but not in all⁴²), though confounding factors such as tumour purity may influence these observations. In addition, the K_M for D-2HG production of the $IDH1^{R132H}$ mutation is higher than that of other *IDH1* mutations (though the enzymatic efficiency may be similar for some mutations)¹⁷. Although we did not directly measure D-2HG levels, the partial inhibition of TET2, may explain the lower overall methylation in $IDH1^{R132H}$ -mutated tumours.

The improved outcome of non-R132H mutated astrocytomas may be explained by a reduced expression of genes that support tumour growth and/or induce treatment sensitivity caused by the increase in CpG methylation. Evidence supporting this hypothesis is the observation that many of the differentially expressed genes are involved in pathways associated with cancer. However, the improved outcome of non-R132H mutated astrocytomas may also be related to the observation that D-2HG is toxic to cells, though only at high concentrations. For example, we have previously shown that exposure to D-2HG or expression of mutated *IDH* constructs reduced proliferation of cells, both *in-vitro* and *in-vivo*⁴⁵. Later independent studies largely confirmed these observations and also conversely, reduction of D-2HG levels by mutant *IDH* inhibitors increased cell proliferation^{16,46-49}. It should be noted however, that in some preclinical model systems a growth inhibitory effect of *IDH*-inhibitors was observed^{50,51}. Functional experiments should confirm this hypothesis. Alternatively, differences in genetic stress and related mutational signatures may also explain the differential distribution of mutations in *IDH*^{32,52}.

Limitations of this study include the relatively small sample size of several datasets, especially those with diagnosis other than the non-1p/19q codeleted gliomas. In addition, the absence of D-2HG level data limits the exploration of a direct correlation between *IDH1/2* mutation type and genome-wide DNA methylation.

In short, we described the effect of *IDH1/2* mutation type on patient outcome and the strong correlation between these specific mutations and genome-wide DNA methylation status. Our observation that non-R132H-mutated 1p/19q non-codeleted gliomas have a more favourable prognosis than their *IDH1*^{R132H} mutated counterpart is clinically relevant and should be taken into account for patient prognostication.

Acknowledgements

The CATNON study was funded by Merck, Sharp and Dohme, and the Brain Tumor Group. The genome-wide DNA methylation profiles study was funded by grant GN-000577 from The Brain Tumour Charity, grant 10685 from the Dutch Cancer Society, financial support from the Vereniging Heino 'Strijd van Salland', and grant CA170278 from the United States Department of Defence. The authors thank the European Organization for Research and Treatment of Cancer for permission to use the data from EORTC studies 26053/22054 (CATNON) and 26091 (TAVAREC) for this research.

Author contributions

Conceptualization: PJF

Methodology: CMT, YH, PJF

Validation: CMT

Investigation CMT, WRV, IdH, MdW, LB, PJF

Resources: MS, WT, PMC, WW, AAB, JFV, OLC, HW, SG, MG, LR, RR, MW, CMcB, JR, RHE, FC, TL, SC, AG, EL, FdV, PJM, MJBT, SV, JO, JVMGB, SE, MAV, AKN, WPM, JMK, PW, KA, RBJ, HJD, BB, VG, MvdB

Data curation CMT, TG, PJF

Writing-original draft: CMT, WRV, MvdB, PJF

Writing-review and editing: all authors

Visualization: CMT, PJF

Supervision: MvdB, PJF

Competing interests

MS reports research grants from Astra-Zeneca, travel grant from Abbvie, personal fees from Genenta, outside the submitted work, PM reports support to attend conferences from BMS and an award towards an investigator initiated study from BMS. BB reports a MERCK grant for the EORTC22033 IGG study. MAV has indirect equity interest and royalty rights from Infuseon Therapeutics, Inc. He has received honoraria from Tocagen, Cellinta, and Celgene. None of these interests overlap with the research presented in this manuscript. Wolfgang Wick receives trial funding from Apogenix, Boehringer Ingelheim, Pfizer and Roche to the institution. He serves on advisory boards for Agios, Bayer, MSD, Novartis, Roche with compensation paid to the institution. MJvdB reports grants from Dutch Cancer Foundation, grants from Brain Tumor Charity, grants from Strijd van Salland, grants from MSD formerly Schering Plough, during the conduct of the study; personal fees from Carthera, personal fees from Nerviano, personal fees from Bayer, personal fees from Celgene, personal fees from Agios, personal fees from Abbvie, personal fees from Karyopharm, personal fees from Boston Pharmaceuticals, personal fees from Genenta, outside the submitted work. AN received research funding from Astra Zeneca, and Douglas Pharmaceuticals, consultancies for Bayer, Roche, Boehringer Ingelheim, MSD, Douglas Pharmaceuticals, Pharmabcine, Atara biotherapeutics, Trizell and Seagen. MW has received research grants from Abbvie, AdastrA, Merck, Sharp & Dohme (MSD), Merck (EMD), Novocure and Quercis, and honoraria for lectures or advisory board participation or consulting from Abbvie, AdastrA, Basilea, Bristol Meyer Squibb (BMS), Celgene, Medac, Merck, Sharp & Dohme (MSD), Merck (EMD), Nerviano Medical Sciences, Novartis, Orbus, Philogen, Roche and Tocagen. FdV reports support from AbbVie, Bioclin Therapeutics, BMS, GSK, Novartis, Octimed Oncology and Vaximm, outside the submitted work. PC reports support from BMS, AbbVie, Merck Serono, MSD, Vifor Pharma,

Daiichi Sankyo, Leo Pharma and Astra Zeneca, outside the submitted work. PJF reports grants from Dutch Cancer Foundation, the Brain Tumor Charity, the Strijd van Salland, de Westlandse ride and Hersentumorfonds, outside submitted work. Other authors report no conflict of interest.

References

1. Clark O, Yen K, Mellingshoff IK. Molecular Pathways: Isocitrate Dehydrogenase Mutations in Cancer. *Clin Cancer Res.* 2016; 22(8): 1837-1842
2. Mito JK, Bishop JA, Sadow PM, et al. Immunohistochemical Detection and Molecular Characterization of IDH-mutant Sinonasal Undifferentiated Carcinomas. *Am J Surg Pathol.* 2018; 42(8): 1067-1075
3. Zehir A, Benayed R, Shah RH, et al. Mutational landscape of metastatic cancer revealed from prospective clinical sequencing of 10,000 patients. *Nature medicine.* 2017; 23(6): 703-713
4. Hirata M, Sasaki M, Cairns RA, et al. Mutant IDH is sufficient to initiate enchondromatosis in mice. *Proc Natl Acad Sci U S A.* 2015; 112(9): 2829-2834
5. Sasaki M, Knobbe CB, Munger JC, et al. IDH1(R132H) mutation increases murine haematopoietic progenitors and alters epigenetics. *Nature.* 2012;
6. Stein EM, DiNardo CD, Pollyea DA, et al. Enasidenib in mutant IDH2 relapsed or refractory acute myeloid leukemia. *Blood.* 2017; 130(6): 722-731
7. DiNardo CD, Stein EM, de Botton S, et al. Durable Remissions with Ivosidenib in IDH1-Mutated Relapsed or Refractory AML. *N Engl J Med.* 2018; 378(25): 2386-2398
8. Abou-Alfa GK, Macarulla T, Javle MM, et al. Ivosidenib in IDH1-mutant, chemotherapy-refractory cholangiocarcinoma (ClarIDHy): a multicentre, randomised, double-blind, placebo-controlled, phase 3 study. *Lancet Oncol.* 2020; 21(6): 796-807
9. Mellingshoff IK, Ellingson BM, Touat M, et al. Ivosidenib in Isocitrate Dehydrogenase 1-Mutated Advanced Glioma. *J Clin Oncol.* 2020; JCO1903327
10. Kloosterhof NK, Bralten LB, Dubbink HJ, French PJ, van den Bent MJ. Isocitrate dehydrogenase-1 mutations: a fundamentally new understanding of diffuse glioma? *Lancet Oncol.* 2011; 12(1): 83-91
11. Gagne LM, Boulay K, Topisirovic I, Huot ME, Mallette FA. Oncogenic Activities of IDH1/2 Mutations: From Epigenetics to Cellular Signaling. *Trends Cell Biol.* 2017; 27(10): 738-752
12. Losman JA, Kaelin WG, Jr. What a difference a hydroxyl makes: mutant IDH, (R)-2-hydroxyglutarate, and cancer. *Genes Dev.* 2013; 27(8): 836-852
13. Pansuriya TC, van Eijk R, d'Adamo P, et al. Somatic mosaic IDH1 and IDH2 mutations are associated with enchondroma and spindle cell hemangioma in Ollier disease and Maffucci syndrome. *Nat Genet.* 2011; 43(12): 1256-1261
14. Gravendeel LA, Kloosterhof NK, Bralten LB, et al. Segregation of non-p.R132H mutations in IDH1 in distinct molecular subtypes of glioma. *Hum Mutat.* 2010; 31(3): E1186-1199
15. Farshidfar F, Zheng S, Gingras MC, et al. Integrative Genomic Analysis of Cholangiocarcinoma Identifies Distinct IDH-Mutant Molecular Profiles. *Cell Rep.* 2017; 18(11): 2780-2794
16. Pusch S, Schweizer L, Beck AC, et al. D-2-Hydroxyglutarate producing neo-enzymatic activity inversely correlates with frequency of the type of isocitrate dehydrogenase 1 mutations found in glioma. *Acta Neuropathol Commun.* 2014; 2(1): 19
17. Avellaneda Matteo D, Grunseth AJ, Gonzalez ER, et al. Molecular mechanisms of isocitrate dehydrogenase 1 (IDH1) mutations identified in tumors: The role of size and hydrophobicity at residue 132 on catalytic efficiency. *J Biol Chem.* 2017; 292(19): 7971-7983
18. Gross S, Cairns RA, Minden MD, et al. Cancer-associated metabolite 2-hydroxyglutarate accumulates in acute myelogenous leukemia with isocitrate dehydrogenase 1 and 2 mutations. *The Journal of experimental medicine.* 2010; 207(2): 339-344
19. Jin G, Reitman ZJ, Spasojevic I, et al. 2-hydroxyglutarate production, but not dominant negative function, is conferred by glioma-derived NADP-dependent isocitrate dehydrogenase mutations. *PLoS ONE.* 2011; 6(2): e16812
20. Chowdhury R, Yeoh KK, Tian YM, et al. The oncometabolite 2-hydroxyglutarate inhibits histone lysine demethylases. *EMBO reports.* 2011; 12(5): 463-469
21. Xu W, Yang H, Liu Y, et al. Oncometabolite 2-Hydroxyglutarate Is a Competitive Inhibitor of alpha-Ketoglutarate-Dependent Dioxygenases. *Cancer Cell.* 2011; 19(1): 17-30

22. van den Bent MJ, Baumert B, Erridge SC, et al. Interim results from the CATNON trial (EORTC study 26053-22054) of treatment with concurrent and adjuvant temozolomide for 1p/19q non-co-deleted anaplastic glioma: a phase 3, randomised, open-label intergroup study. *Lancet*. 2017; 390(10103): 1645-1653
23. Ceccarelli M, Barthel FP, Malta TM, et al. Molecular Profiling Reveals Biologically Discrete Subsets and Pathways of Progression in Diffuse Glioma. *Cell*. 2016; 164(3): 550-563
24. van den Bent MJ, Klein M, Smits M, et al. Bevacizumab and temozolomide in patients with first recurrence of WHO grade II and III glioma, without 1p/19q co-deletion (TAVAREC): a randomised controlled phase 2 EORTC trial. *Lancet Oncol*. 2018; 19(9): 1170-1179
25. Tyner JW, Tognon CE, Bottomly D, et al. Functional genomic landscape of acute myeloid leukaemia. *Nature*. 2018; 562(7728): 526-531
26. Cheng DT, Mitchell TN, Zehir A, et al. Memorial Sloan Kettering-Integrated Mutation Profiling of Actionable Cancer Targets (MSK-IMPACT): A Hybridization Capture-Based Next-Generation Sequencing Clinical Assay for Solid Tumor Molecular Oncology. *The Journal of molecular diagnostics : JMD*. 2015; 17(3): 251-264
27. Suzuki H, Aoki K, Chiba K, et al. Mutational landscape and clonal architecture in grade II and III gliomas. *Nat Genet*. 2015;
28. Killela PJ, Reitman ZJ, Jiao Y, et al. TERT promoter mutations occur frequently in gliomas and a subset of tumors derived from cells with low rates of self-renewal. *Proc Natl Acad Sci U S A*. 2013; 110(15): 6021-6026
29. Hu H, Mu Q, Bao Z, et al. Mutational Landscape of Secondary Glioblastoma Guides MET-Targeted Trial in Brain Tumor. *Cell*. 2018; 175(6): 1665-1678 e1618
30. Aryee MJ, Jaffe AE, Corrada-Bravo H, et al. Minfi: a flexible and comprehensive Bioconductor package for the analysis of Infinium DNA methylation microarrays. *Bioinformatics*. 2014; 30(10): 1363-1369
31. Forbes SA, Beare D, Boutselakis H, et al. COSMIC: somatic cancer genetics at high-resolution. *Nucleic Acids Res*. 2017; 45(D1): D777-D783
32. Alexandrov LB, Kim J, Haradhvala NJ, et al. The repertoire of mutational signatures in human cancer. *Nature*. 2020; 578(7793): 94-101
33. Losman JA, Koivunen P, Kaelin WG, Jr. 2-Oxoglutarate-dependent dioxygenases in cancer. *Nat Rev Cancer*. 2020;
34. de Souza CF, Sabedot TS, Malta TM, et al. A Distinct DNA Methylation Shift in a Subset of Glioma CpG Island Methylator Phenotypes during Tumor Recurrence. *Cell Rep*. 2018; 23(2): 637-651
35. Noushmehr H, Weisenberger DJ, Diefes K, et al. Identification of a CpG island methylator phenotype that defines a distinct subgroup of glioma. *Cancer Cell*. 2010; 17(5): 510-522
36. Kloosterhof NK, de Rooij JJ, Kros M, et al. Molecular subtypes of glioma identified by genome-wide methylation profiling. *Genes Chromosomes Cancer*. 2013; 52(7): 665-674
37. Capper D, Jones DTW, Sill M, et al. DNA methylation-based classification of central nervous system tumours. *Nature*. 2018; 555(7697): 469-474
38. van den Bent MJ, Gravendeel LA, Gorlia T, et al. A hypermethylated phenotype is a better predictor of survival than MGMT methylation in anaplastic oligodendroglial brain tumors: a report from EORTC study 26951. *Clin Cancer Res*. 2011; 17(22): 7148-7155
39. Spainhour JC, Lim HS, Yi SV, Qiu P. Correlation Patterns Between DNA Methylation and Gene Expression in The Cancer Genome Atlas. *Cancer Inform*. 2019; 18(1176935119828776
40. Natsumeda M, Igarashi H, Nomura T, et al. Accumulation of 2-hydroxyglutarate in gliomas correlates with survival: a study by 3.0-tesla magnetic resonance spectroscopy. *Acta Neuropathol Commun*. 2014; 2(158
41. Franceschi E, De Biase D, Pession A, et al. Survival outcomes in glioma patients with noncanonical IDH mutations: Beyond diagnostic improvements. *J Clin Oncol*. 2019; 37(15 (suppl)): 2028

42. Choi C, Ganji SK, DeBerardinis RJ, et al. 2-hydroxyglutarate detection by magnetic resonance spectroscopy in IDH-mutated patients with gliomas. *Nature medicine*. 2012; 18(4): 624-629
43. Longuespee R, Wefers AK, De Vita E, et al. Rapid detection of 2-hydroxyglutarate in frozen sections of IDH mutant tumors by MALDI-TOF mass spectrometry. *Acta Neuropathol Commun*. 2018; 6(1): 21
44. Kanamori M, Maekawa M, Shibahara I, et al. Rapid detection of mutation in isocitrate dehydrogenase 1 and 2 genes using mass spectrometry. *Brain Tumor Pathol*. 2018; 35(2): 90-96
45. Bralten LB, Kloosterhof NK, Balvers R, et al. IDH1 R132H decreases proliferation of glioma cell lines in vitro and in vivo. *Ann Neurol*. 2011; 69(3): 455-463
46. Pickard AJ, Sohn AS, Bartenstein TF, et al. Intracerebral Distribution of the Oncometabolite d-2-Hydroxyglutarate in Mice Bearing Mutant Isocitrate Dehydrogenase Brain Tumors: Implications for Tumorigenesis. *Front Oncol*. 2016; 6(211)
47. Tateishi K, Wakimoto H, Iafrate AJ, et al. Extreme Vulnerability of IDH1 Mutant Cancers to NAD⁺ Depletion. *Cancer Cell*. 2015; 28(6): 773-784
48. Fu X, Chin RM, Vergnes L, et al. 2-Hydroxyglutarate Inhibits ATP Synthase and mTOR Signaling. *Cell Metab*. 2015; 22(3): 508-515
49. Zhang Y, Pusch S, Innes J, et al. Mutant IDH Sensitizes Gliomas to Endoplasmic Reticulum Stress and Triggers Apoptosis via miR-183-Mediated Inhibition of Semaphorin 3E. *Cancer Res*. 2019; 79(19): 4994-5007
50. Rohle D, Popovici-Muller J, Palaskas N, et al. An inhibitor of mutant IDH1 delays growth and promotes differentiation of glioma cells. *Science*. 2013; 340(6132): 626-630
51. Pusch S, Krausert S, Fischer V, et al. Pan-mutant IDH1 inhibitor BAY 1436032 for effective treatment of IDH1 mutant astrocytoma in vivo. *Acta Neuropathol*. 2017; 133(4): 629-644
52. Alexandrov LB, Nik-Zainal S, Wedge DC, et al. Signatures of mutational processes in human cancer. *Nature*. 2013; 500(7463): 415-421

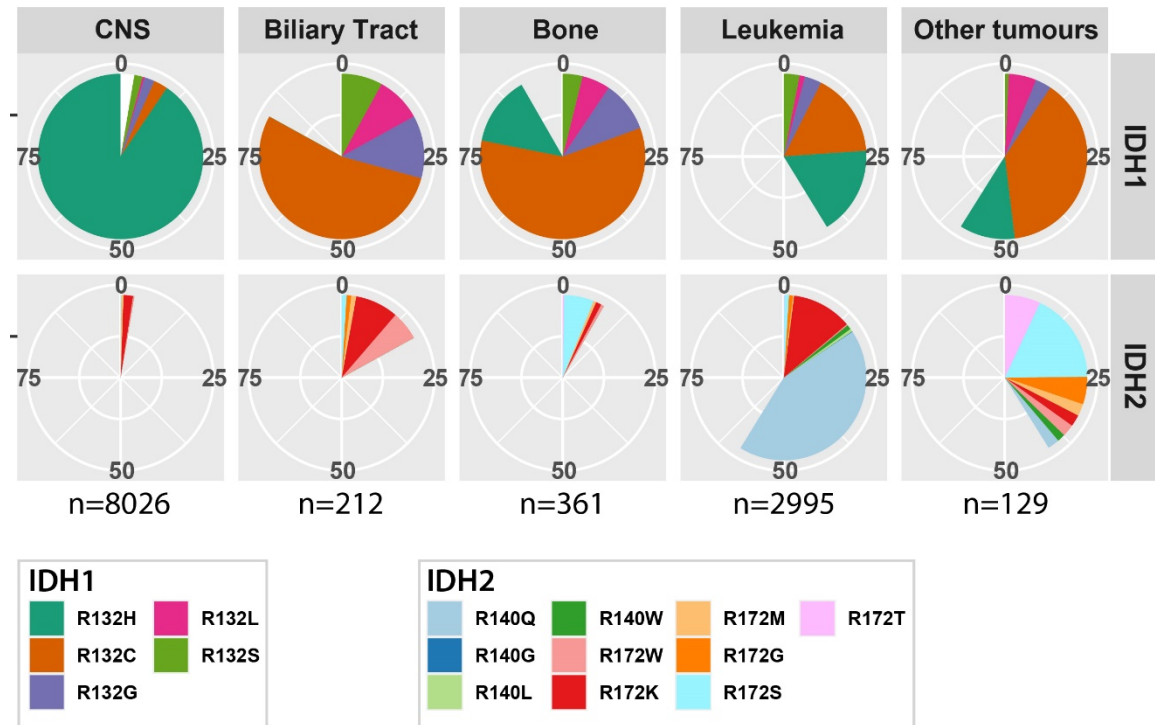


Figure 1: *IDH1* and *IDH2* hotspot mutation distribution separated by site of origin. $IDH1^{R132H}$ mutations are the most predominant mutation in gliomas, *IDH2* mutations are most common to haematopoietic tumours.

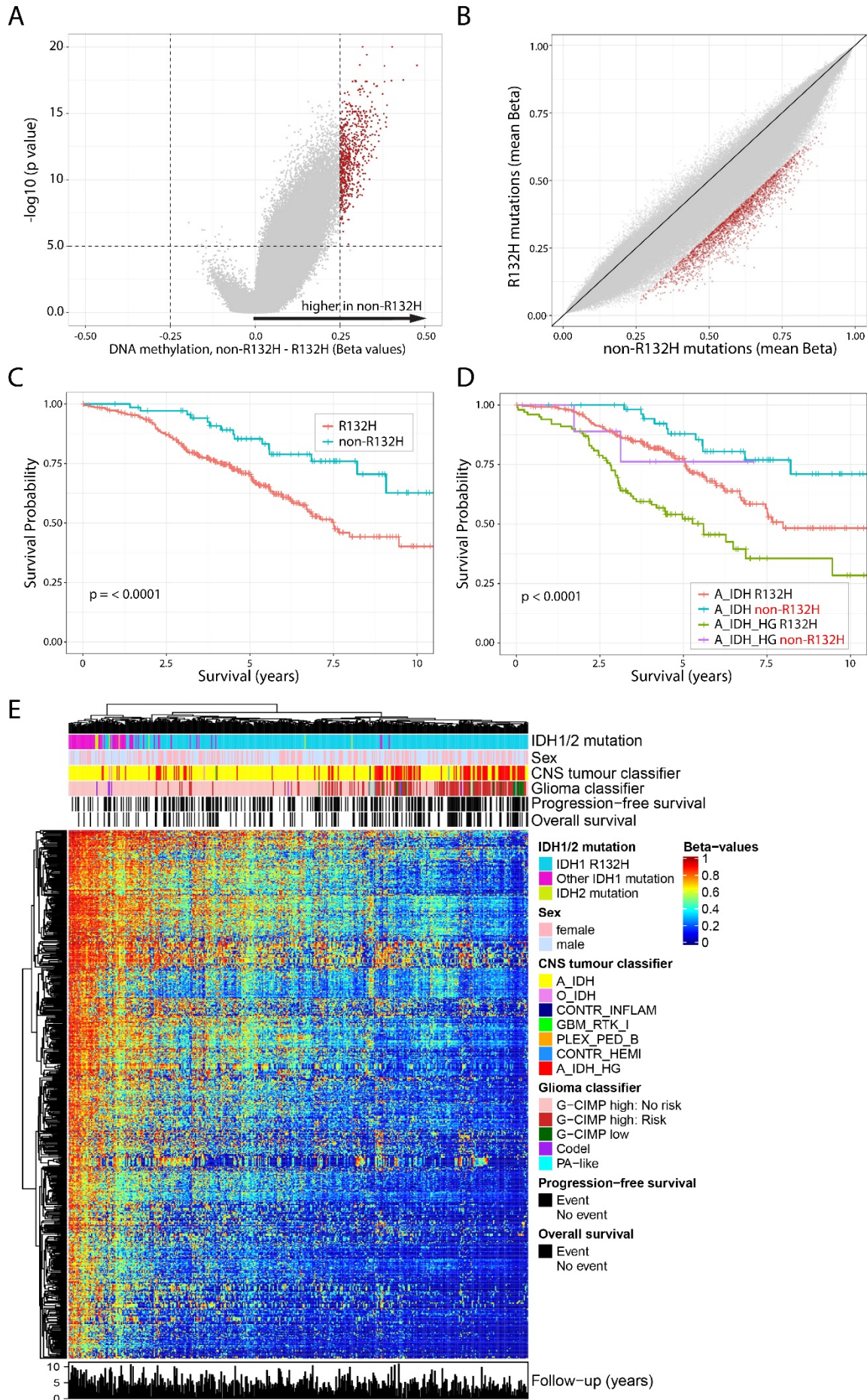


Figure 2: non-R132H mutations are associated with higher DNA methylation levels and improved survival of 1p19q non-codeleted astrocytoma patients included in the CATNON trial. Volcano plot (A) and XY plot (B) showing differences in methylation in non-R132H v. IDH1^{R132H} mutated tumours. C) patients harbouring non-R132H mutated tumours have improved outcome, which is independent of methylation class (D). Heatmap of the most differentially methylated probes (red dots in A and B), shows a gradient in methylation levels. Non-R132H mutated tumours cluster at the far left (high methylation), where poor prognostic methylation subtypes (epigenetics subtypes) cluster at the opposite end.

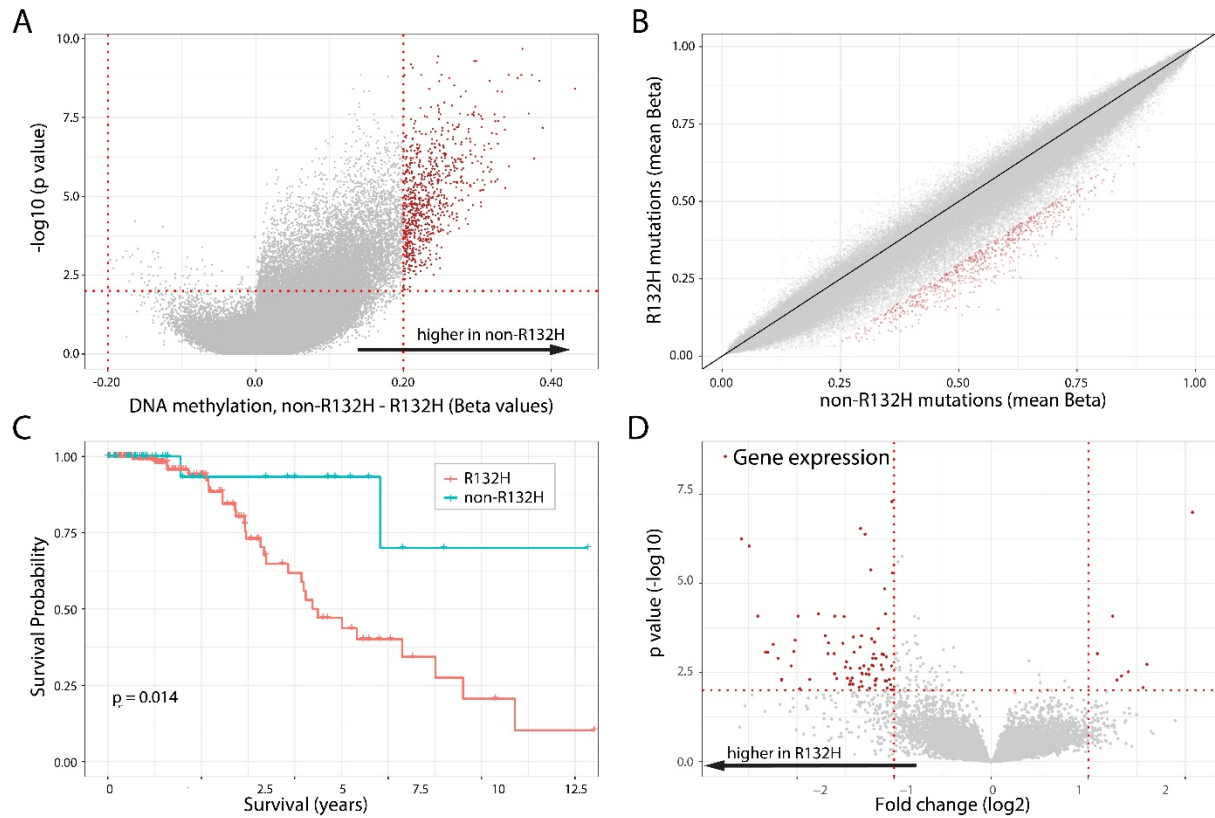


Figure 3: non-R132H mutations are associated with higher DNA methylation levels, lower gene expression and improved survival of 1p19q non-codeleted astrocytoma patients of the TCGA. Volcanoplot (A) and XY plot (B) showing differences in methylation in non-R132H v. IDH1^{R132H} mutated tumours. C) patients harbouring non-R132H mutated tumours have improved outcome. (D) Volcanoplot showing differential expression of genes between non-R132H and IDH1^{R132H} mutated tumours. Most differentially expressed genes (red dots) have lower expression in non-R132H mutated tumours (see also supplementary table 2).

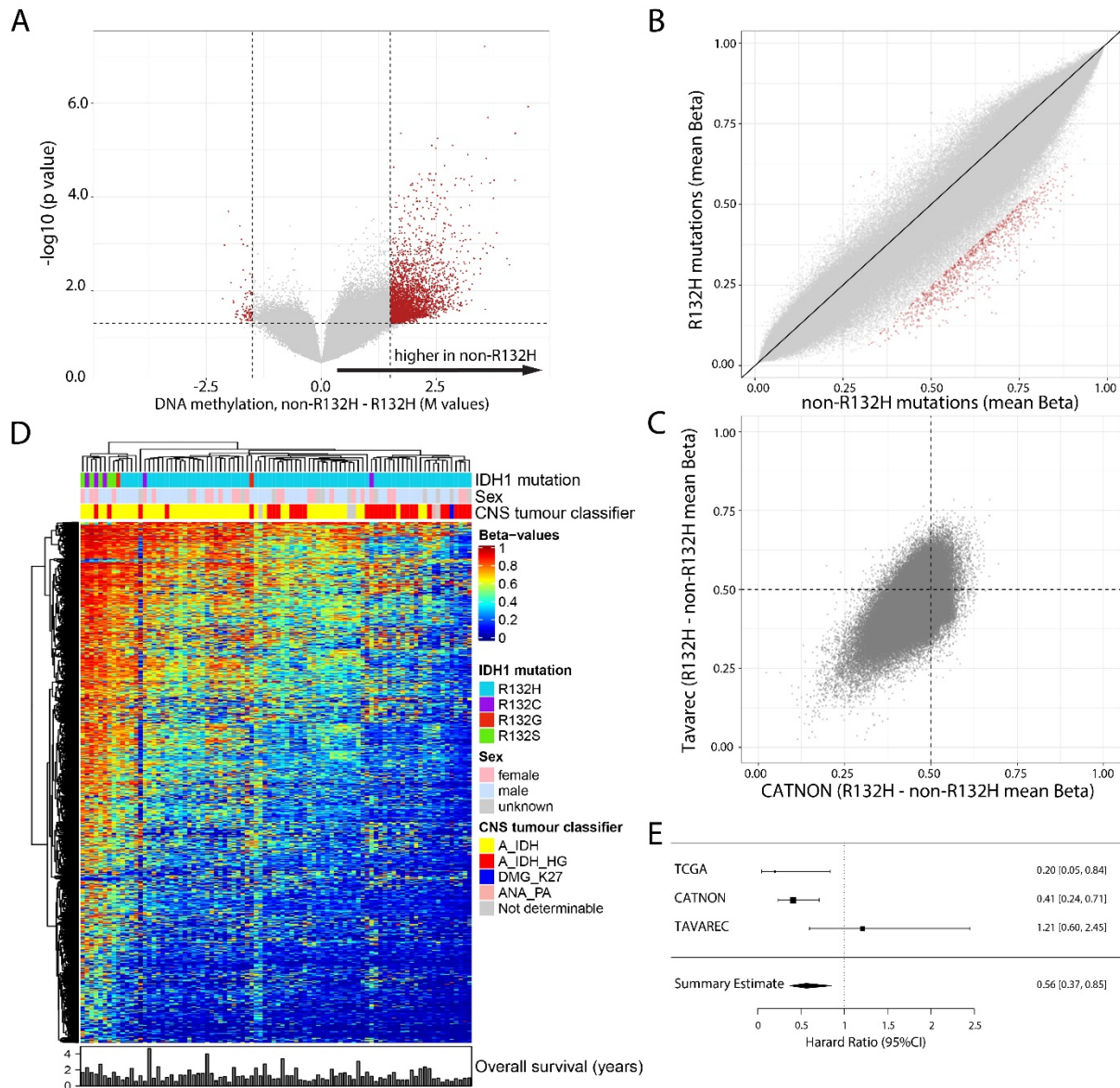


Figure 4: non-R132H mutations are associated with higher DNA methylation levels in 1p19q non-codeleted astrocytoma samples of patients included in the Tavarec trial. Volcanoplot (A) and XY plot (B) showing differences in methylation in non-R132H v. IDH1^{R132H} mutated tumours. C) Differential methylation between non-R132H v. IDH1^{R132H} mutated tumours showed a large degree of overlap in CATNON (x axis) and Tavarec (y axis) samples. (D) Heatmap of the most differentially methylated probes (red dots in A and B), shows a gradient in methylation levels. Non-R132H mutated tumours cluster at the far left (high methylation), where poor prognostic methylation subtypes (epigenetics subtypes) cluster at the opposite end. E) Forrest plot showing the summary HR estimate of 1p19q non-codeleted astrocytoma patients harbouring non-R132H v. IDH1^{R132H} mutated tumours.

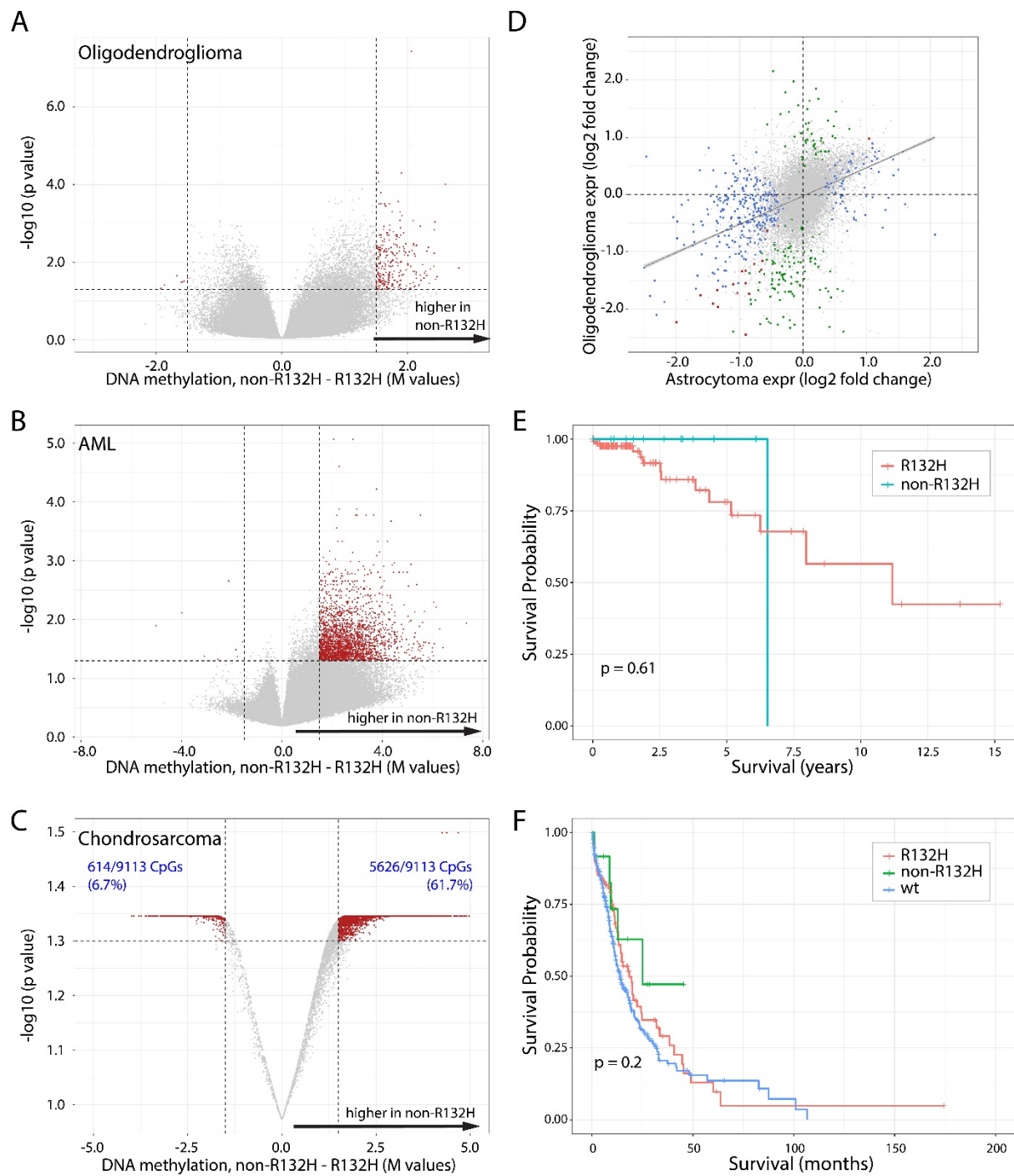
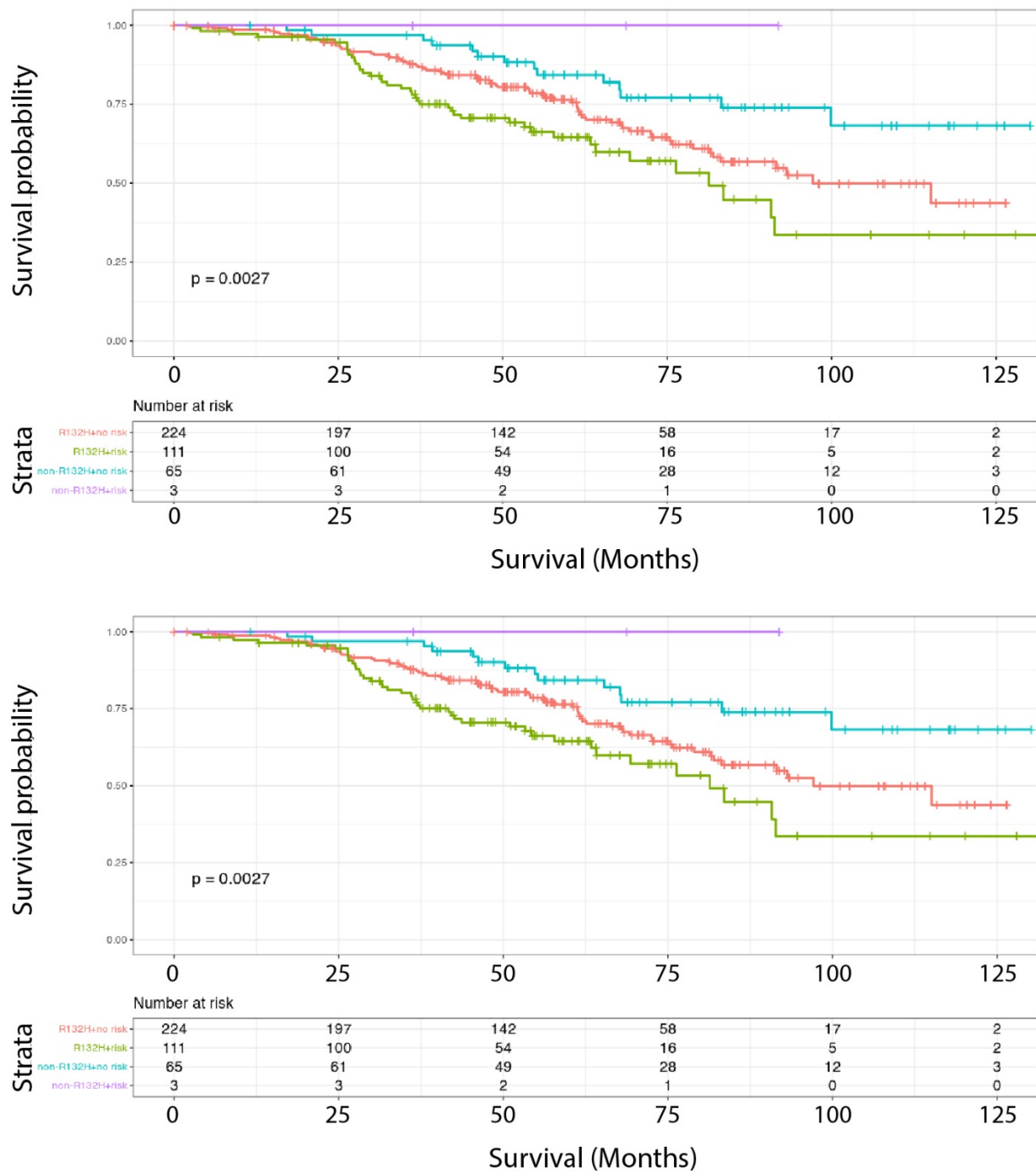


Figure 5: non-R132H mutations are associated with higher DNA methylation levels independent of tumour type. Volcanoplots of 1p19q codeleted oligodendrogliomas (A), AML (B) and chondrosarcomas (C) showing differences in methylation in non-R132H v. IDH1^{R132H} mutated tumours. Red dots depict CpGs that had a >0.2 change in beta value, and were significant ($P < 0.01$) in a Wilcoxon rank test (in B and C, the Y-axis are t-test P-values for visualization purposes). Although the difference in chondrosarcomas is less than in other tumour types, the majority of significant CpGs was in non-R132H-mutated tumours (e.g. 225 CpG showed a >0.3 increase in beta value at $p < 0.01$ where only 47 showed a similar decrease). D) Gene expression differences between non-R132H v. IDH1^{R132H} mutated tumours in 1p19q non-codeleted astrocytomas (x-axis) and 1p19q codeleted oligodendrogliomas (y-axis) shows a large degree of overlap. Blue, green and red dots

depict genes significantly differentially expressed in astrocytomas, oligodendrogliomas or both respectively (see also supplementary table 2 and 3). E). Survival of 1p19q codeleted oligodendroglioma patients present in the TCGA database harbouring non-R132H v. IDH1^{R132H} mutated tumours. There were too few events evaluate survival differences per mutation type. F) mutation type-specific survival differences in AML.

Table 1. Multivariable model

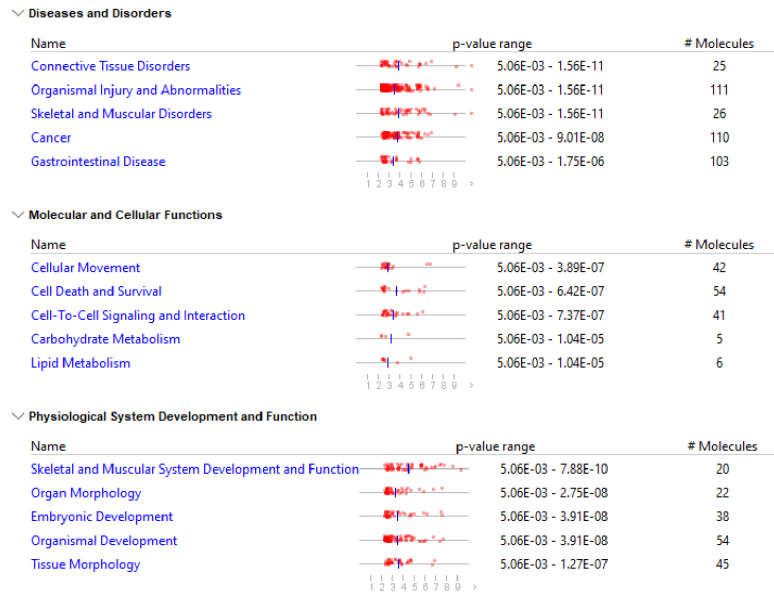
		HR	95% CI		p value
IDH mutation type	non-R132H v. R132H	0.486	0.278	0.852	0.012
Sex	Male v. Female	1.465	1.033	2.076	0.032
Treatment	RT->TMZ v. RT	0.410	0.257	0.653	0.000
	TMZ/RT v. RT	0.802	0.520	1.237	0.319
	TMZ/RT->TMZ v. RT	0.385	0.231	0.639	0.000
Age	40-60 v. <40 years	1.121	0.656	1.914	0.677
	>60 v. < 40 years	3.824	1.812	8.069	0.000
Performance score	1 v. 0	1.404	0.991	1.990	0.056
	2 v. 0	2.282	0.704	7.401	0.169
MGMT promoter methylation	UM v. M	1.001	0.640	1.567	0.996
Corticosteroid use	Yes v. No	1.099	0.742	1.627	0.639
Methylation subtype	A_IDH_HG v. A_IDH	2.650	1.828	3.842	0.000
	O_IDH v. A_IDH	0.362	0.083	1.584	0.177
	other v. A_IDH	10.763	3.410	33.970	0.000



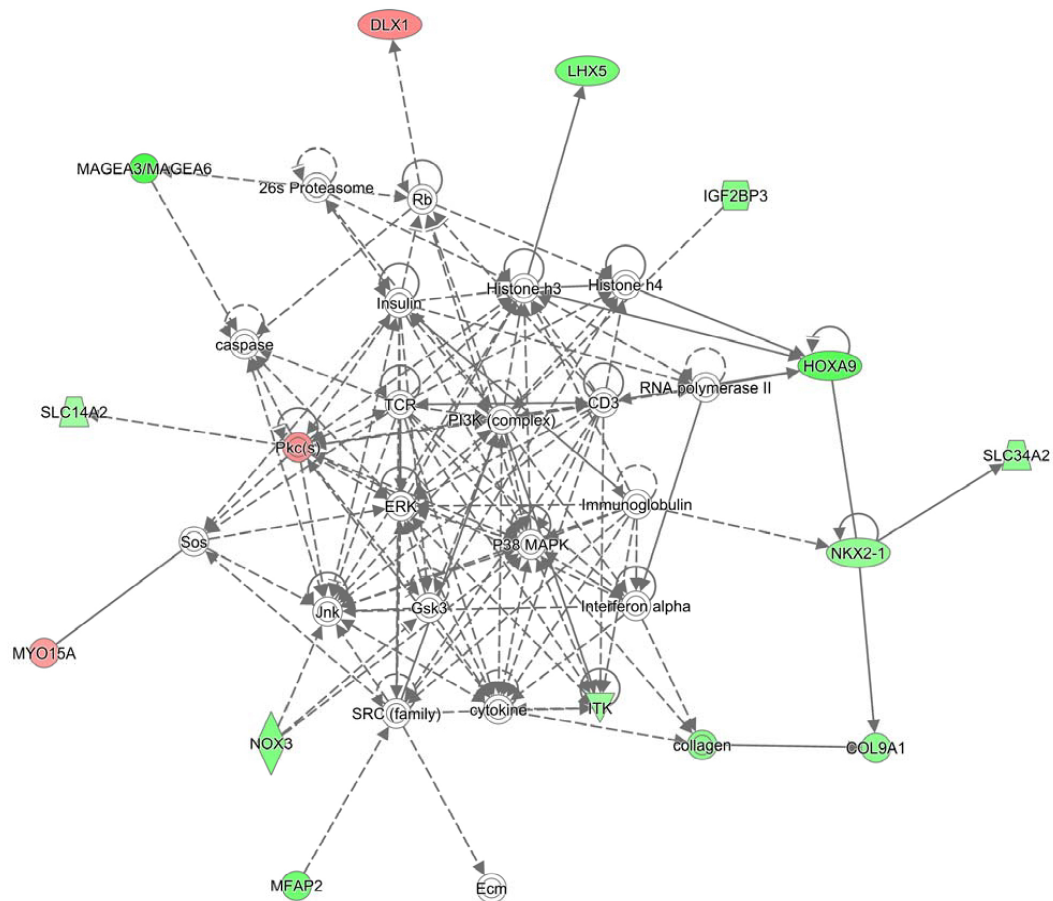
Supplementary figure 1: non-R132H mutations are associated with improved survival of 1p19q non-codeleted astrocytoma patients included in the CATNON trial independent of methylation class.

Survival of patients harbouring non-R132H or IDH1^{R132H} mutated tumours stratified by methylation class as defined by the TCGA (top) or risk to G-CIMP-low progression (bottom). As can be seen, patients harbouring non-R132H mutated tumours have improved outcome, independent of methylation class.

A



B



Supplementary figure 2: Pathway analysis of genes differentially expressed between non-R132H and *IDH1*^{R132H} mutated tumours. A) top diseases and disorders, molecular and cellular functions and physiological system development and function identified by pathway analysis. B) graphical representation of the top cancer pathway.

Supplementary table 1

		HR	95% CI		p value
IDH mutation type	non-R132H v. R132H	0.378	0.217	0.659	0.0006
Sex	Male v. Female	1.377	0.978	1.939	0.067
Treatment	RT->TMZ v. RT	0.485	0.307	0.768	0.002
	TMZ/RT v. RT	0.734	0.479	1.124	0.154
	TMZ/RT->TMZ v. RT	0.432	0.266	0.703	0.0007
Age	40-60 v. <40 years	1.021	0.598	1.744	0.94
	>60 v. < 40 years	2.413	1.188	4.903	0.015
Performance score	1 v. 0	1.455	1.030	2.055	0.033
	2 v. 0	1.732	0.540	5.563	0.36
MGMT promoter methylation	UM v. M	1.092	0.715	1.668	0.68
Corticosteroid use	Yes v. No	1.312	0.895	1.925	0.16

Supplementary table 2

		HR	95% CI		p value
IDH mutation type	non-R132H v. R132H	0.429	0.245	0.751	0.003
Sex	Male v. Female	1.393	0.985	1.971	0.061
Treatment	RT->TMZ v. RT	0.443	0.280	0.703	0.001
	TMZ/RT v. RT	0.744	0.484	1.144	0.178
	TMZ/RT->TMZ v. RT	0.441	0.267	0.728	0.001
Age	40-60 v. <40 years	1.167	0.679	2.004	0.577
	>60 v. < 40 years	3.082	1.483	6.407	0.003
Performance score	1 v. 0	1.501	1.057	2.130	0.023
	2 v. 0	1.989	0.617	6.410	0.250
MGMT promoter methylation	UM v. M	0.970	0.627	1.500	0.891
Corticosteroid use	Yes v. No	1.271	0.861	1.877	0.228
Methylation subtype	G-CIMP low v G-CIMP high	4.072	2.231	7.430	0.000
	Codel v G-CIMP high	0.417	0.127	1.373	0.150
	PA-like v G-CIMP high	3.609	0.789	16.514	0.098

Supplementary table 3

Gene.name	log2FoldChange
AJ011932.1	-2.737589267
PCDHGB4	-2.571945205
CEACAM5	-2.5341973
SHOX2	-2.492427446
KRT13	-2.460839239
AC104051.2	-2.403250008
IGHV1-18	-2.330831346
HOXA5	-2.323982392
LINC01956	-2.300130233
LINC02513	-2.24479318
NTS	-2.194539237
SIX6	-2.175101096
EN1	-2.158765071
HOXA7	-2.157135213
MAGEA6	-2.071106151
HOXA10	-2.059261084
IL21-AS1	-2.042870083
IBSP	-2.036361159
SCGB3A2	-2.030888599
CCDC198	-2.018895459
MTCYBP18	-1.988541182
HOXD9	-1.97664222
H1-9P	-1.974360534
LINC01993	-1.969448233
AC015909.3	-1.905007912
KRT16	-1.891557269
HOXA9	-1.883361185
TBX5	-1.867429903
H19	-1.801177989
LRRC18	-1.777074293
DLK1	-1.727130873
IDO1	-1.72137244
CNIH3-AS1	-1.719623402
AC096669.1	-1.707462577
SCNN1B	-1.680229048
AC068308.1	-1.675592245
PLEKHS1	-1.656709761
DAO	-1.643293356
MFAP2	-1.616778551
HAGLROS	-1.612619442
LINC01235	-1.611484946
HOXA4	-1.603222266

TBX5-AS1	-1.597762594
CHI3L1	-1.591438123
LHX5	-1.575761551
MIR4527HG	-1.52646164
LINC01485	-1.515218265
AC062021.1	-1.501396095
TRIM71	-1.490465977
SLC17A8	-1.479718763
AC253536.4	-1.460186616
LINC01571	-1.454158719
LCE1E	-1.450018917
NOX3	-1.44740241
AC104574.2	-1.432576878
IL13RA2	-1.426872513
C3orf22	-1.426816188
C2orf91	-1.424551675
AL390755.2	-1.417799432
LINC01579	-1.410814502
PCAT4	-1.408801892
IGF2-AS	-1.407277847
IGF2BP3	-1.394810745
AC008080.4	-1.388244005
ASB11	-1.374324083
AL158058.1	-1.37079861
AC084864.1	-1.360024733
SPOCD1	-1.356355284
HAMP	-1.353158198
TGFB2	-1.350160759
TRPC7	-1.349144827
APOH	-1.34872969
DLGAP1-AS5	-1.345754514
SHISAL2B	-1.340049125
ALPK2	-1.338269773
AC005999.1	-1.335162176
SRD5A2	-1.332787731
AC009097.2	-1.332505081
AC007402.1	-1.327565511
COL9A1	-1.327235013
AEBP1	-1.309900005
SLC34A2	-1.302526748
AC006372.3	-1.29796104
BARHL1	-1.296094493
PLAC8	-1.287968261
LINC01387	-1.271777633
AC061992.2	-1.271585912
AL354811.1	-1.262808675
NKX2-1	-1.258751209

AC008760.2	-1.257935042
ASB5	-1.256795604
PCDHGA3	-1.252469346
FGFBP2	-1.250388105
CXCL10	-1.250319136
SLPI	-1.239113683
LINC00606	-1.230027579
IL21R	-1.229097284
TFAP2A	-1.227993409
IFI6	-1.218666285
S100A3	-1.217530644
ARHGAP36	-1.214660604
AL049839.2	-1.214006748
NA	-1.209976594
PIRT	-1.206189984
VGF	-1.202116275
AC126773.4	-1.200656398
TRPM8	-1.198024209
SLCO4A1-AS1	-1.192055585
SLC18A1	-1.191695755
RPS3AP5	-1.18708919
AC073389.2	-1.183287408
AP005202.1	-1.182697026
TREM1	-1.176000574
ITK	-1.172545553
ULBP1	-1.166387637
HNRNPKP3	-1.162965555
AC107419.1	-1.162344351
ARSF	-1.150883317
LINC02574	-1.150231164
LCE1D	-1.143358674
AC112493.1	-1.14299355
ABCA13	-1.131583881
PTX3	-1.124334869
C10orf105	-1.121615634
LINC02282	-1.120792665
GRHL3-AS1	-1.119249705
AC002546.1	-1.119126233
TIMP4	-1.107649912
FAM151A	-1.097568155
NR1H4	-1.096213209
AC004899.2	-1.091653154
MYBL2	-1.087380276
INSM1	-1.086795726
SLC14A2	-1.080179565
CA9	-1.078361897
SPATA3	-1.077455875

ADAMTS7P4	-1.075366136
AC027281.2	-1.071532654
ADIG	-1.070317119
LINC01224	-1.070240332
LINC02029	-1.069804734
NA	-1.067618019
TMSB15A	-1.067419295
GNLY	-1.063935711
PCDHA7	-1.059616824
CFAP77	-1.048266211
CDC14C	-1.040485693
LINC01349	-1.03912138
AC023421.1	-1.034292301
TNFSF13B	-1.029345357
THEM7P	-1.027307556
MT1F	-1.02610821
LINC02777	-1.021269904
VEPH1	-1.018627595
EYA1	-1.018248945
USP30-AS1	-1.011199972
C21orf62	-1.003904261
MYO15A	1.002369696
REM1	1.036824656
SLCO4C1	1.068178932
AC103681.2	1.075356234
GRM2	1.080043134
CALML3-AS1	1.085922855
OTOF	1.090196171
SGCG	1.092779196
TNIP3	1.104033991
PRKCG	1.129143448
GNG13	1.135341651
FBXO40	1.163078138
TPO	1.188794917
DLX1	1.190730282
CLEC4G	1.194118952
PCDHGB3	1.251510045
S100A7	1.294257769
MTCO3P12	1.341898853
SLC22A9	1.369452854
PRND	1.413607686
PRTN3	1.419613663
KLK7	1.424761311
AC140125.2	1.497638207
CLEC4GP1	1.562749558
SLC38A4	1.603508363
NPIP13	2.072398191

Supplementary table 4

Gene.name	log2FoldChange
MTRNR2L1	-5.520724037
LINC01055	-4.380363929
PITX1	-3.992410842
CCDC198	-3.91584956
TFAP2B	-3.824382791
DAO	-3.704166761
AC068308.1	-3.243847134
CNN2P8	-3.148696973
AC023421.1	-2.916224137
LINC01485	-2.808094538
SLC14A2	-2.798813886
STON1- GTF2A1L	-2.725619928
CCL1	-2.706869245
EN1	-2.62447316
ISL2	-2.597031297
CHIT1	-2.530243103
IL13RA2	-2.505016251
ENOX1-AS2	-2.447615266
AC022498.1	-2.390691554
CHRM5	-2.390294807
PCDHGB1	-2.328605085
PCDHGB6	-2.312015563
SLC14A1	-2.270870574
NMUR2	-2.270733359
SLC47A2	-2.262412923
AL603840.1	-2.248180985
MTCYBP18	-2.224655459
KIF6	-2.223589491
TFCP2L1	-2.193455866
LINC02308	-2.167770915
AL033519.1	-2.136495258
AC091151.1	-1.975602204
AC005999.1	-1.965555734
LINC01894	-1.912781222
LINC01579	-1.9039876
AL355916.2	-1.84043909
SFRP2	-1.839939629
GSX2	-1.835719986
CCL4L2	-1.794607717
NA	-1.778943819
CRLF1	-1.773109087
LINC01235	-1.758861682
AC026316.3	-1.736707567

AL161935.1	-1.732663246
TNFSF13B	-1.723565612
RN7SKP23	-1.713341854
AL355482.1	-1.708920378
TIGIT	-1.697341592
HIRAP1	-1.695118366
LINC00994	-1.693595145
CCL4	-1.689420884
CCL3L1	-1.685923314
DLGAP1-AS5	-1.665873392
SNORC	-1.6651562
IL1B	-1.661839939
THORLNC	-1.652046554
CCL3	-1.647463936
AC092040.2	-1.643428448
TNFSF18	-1.635271455
AC139491.2	-1.630242068
AC068790.1	-1.594647512
PGM5P4	-1.588087948
SALL4	-1.576421413
LPL	-1.574161491
USH1C	-1.56772355
AC092112.1	-1.565593909
FAM151A	-1.564868904
AC091435.2	-1.556627129
FAM181A-AS1	-1.546233218
AC004485.1	-1.533405325
Z84468.1	-1.522085163
CCT7P2	-1.521992916
REELD1	-1.507029939
AP003472.1	-1.501948058
AP000424.1	-1.486411807
AL355974.2	-1.477589802
CALN1	-1.471320426
GFAP	-1.469268554
LINC01736	-1.443494141
TRDN	-1.437372297
AC005162.2	-1.400400857
TLR4	-1.399146112
SLC11A1	-1.389398943
AP004782.1	-1.386916969
AL390755.1	-1.382538868
AL391845.2	-1.373598494
BTC	-1.371751893
AC084880.1	-1.366963829
AC084880.3	-1.363921455
LINC01117	-1.361051862

ACKR4	-1.349531264
FAM184B	-1.343255695
ACOT11	-1.34158337
CH25H	-1.340510059
MIR3151	-1.331716185
LINC01132	-1.312126547
AC093305.1	-1.302303524
AL035665.1	-1.29310018
LINC01933	-1.260115378
LINC01480	-1.257478371
SLC35E1P1	-1.250371519
TEKT3	-1.216363248
TMEM72	-1.210581484
ADGRE4P	-1.209793588
CFAP300	-1.200305634
HOGA1	-1.198967863
GREB1L	-1.188824146
LINC01094	-1.181797216
S100Z	-1.177196503
WARS2-IT1	-1.176083234
PCBP3-AS1	-1.175294791
ELN-AS1	-1.169291966
LINC01354	-1.154376228
TPRG1-AS1	-1.151270415
LINC00877	-1.139144855
L3MBTL4-AS1	-1.12221505
AC093627.7	-1.120734298
LINC02145	-1.106081339
AL157823.2	-1.098547658
RHBDL3	-1.09053745
GYG2	-1.075122004
LRRC37A7P	-1.070713931
KCNJ16	-1.024858397
CAVIN3	1.009076484
LINC02761	1.018693732
CSAG1	1.059398456
ADAMTSL5	1.069855548
HPGD	1.12645928
FGF18	1.143058008
PLEKHG4	1.149908695
MYL9	1.1897534
TFPI	1.2233101
FOXS1	1.236144832
COX4I2	1.249191043
SPON2	1.28821644
PXDNL	1.404933681
FSCN2	1.444151007

AL109615.3	1.446914523
FMO1	1.492060237
CNN1	1.558405106
GJA5	1.635759646
SV2C	1.67050452
MYOCD	1.781451983
DES	1.845422778
LRRC36	1.969650897
MYH11	2.157843483
PCDHGA6	2.7791885
SLC22A8	2.917933903